# AIAA 02-3627

## INITIATION SYSTEMS FOR PULSE DETONATION ENGINES

S. I. Jackson and J.E. Shepherd
*Graduate Aeronautical Laboratories,*
*California Institute of Technology, Pasadena, CA 91125*

**38th AIAA/ASME/SAE/ASEE**
**Joint Propulsion Conference and Exhibit**
**July 7-10, 2002, Indianapolis, IN**

# INITIATION SYSTEMS FOR PULSE DETONATION ENGINES

S. I. Jackson and J.E. Shepherd
*Graduate Aeronautical Laboratories,*
*California Institute of Technology, Pasadena, CA 91125*

**A device capable of creating a collapsing toroidal detonation wave front has been designed and constructed. The goal is to generate pressures and temperatures at the focal region of the collapsing detonation wave that will be sufficient to initiate detonations in insensitive fuel-air mixtures inside of a detonation tube without blocking the flow path and causing associated losses in propulsive efficiency. This toroidal initiator uses a single spark and an array of small-diameter channels to generate and merge many detonation waves to create a single detonation wave with a toroidal front.**

**The development process of the initiator system is described. Steps investigated involve detonation propagation through small tubes, development of a planar initiator capable of initiating a planar detonation wave from a single weak spark, and design and testing of the toroidal initiator. Results presented include the temporal history of pressure at locations near the focus of the collapsing torus and images of the front luminosity. The symmetry of the implosion and practical considerations related to repetitive operation are discussed.**

## Nomenclature

| | |
|---|---|
| $A$ | surface area of the detonation wave |
| $D$ | Chapman-Jouguet (CJ) detonation wave velocity |
| $P$ | pressure of the imploding wave |
| $P_i$ | initial pressure of reactants |
| $P_1$ | initial pressure in computation |
| $P_2$ | post-shock pressure in computation |
| $P_{CJ}$ | pressure at CJ condition |
| $Q$ | heat release at the detonation front per unit mass |
| $T_1$ | initial temperature in computation |
| $T_2$ | post-shock temperature in computation |
| $R_i$ | radius of detonation wave at CJ conditions |
| $R_s$ | instantaneous detonation wave radius |
| $\dot{R}_s$ | instantaneous detonation wave velocity |
| $u$ | initial particle velocity of reactants |
| $u_i$ | particle velocity of the imploding wave |
| $\alpha$ | detonation wave speed parameter, Eq. (2) |
| $\gamma$ | ratio of specific heats in mixture reactants |
| $\rho$ | density of the imploding wave |
| $\rho_i$ | initial density of reactants |
| $\theta$ | angle along toroidal wave front |

## Introduction

RECENTLY, there has been significant interest[1,2] in developing efficient methods of initiating detonations in insensitive fuel-air mixtures (such as JP10 and air, or propane and air) for air breathing pulse detonation engine (PDE) applications. A necessary step in moving from laboratory demonstrations to actual propulsion systems is the development of a device capable of efficiently generating the pressures and temperatures necessary to initiate detonations in these mixtures. One such method involves detonation wave focusing. In detonation wave focusing, a collapsing detonation wave generates a high-pressure and temperature focal region by adiabatically compressing products as they flow into an ever-decreasing area. The compression increases the post-detonation wave pressure higher than the Chapman-Jouguet (CJ) pressure, resulting in an increasingly overdriven detonation wave.

It is desirable to develop a system capable of initiating detonations in hydrocarbon-air mixtures with a low energy spark (less than 100 mJ) for use in short-length, small-diameter detonation tubes. The use of low spark energy eliminates the possibility of direct initiation of detonations in the mixtures of interest. Previous investigations in our group have focused on the potential of several initiation concepts requiring low energy input, such as deflagration to detonation transition (DDT), use of driver or pre-detonator tubes, and detonation wave focusing techniques. Each concept was evaluated for use with PDEs.

Experiments[3] involving direct impulse measurements of detonation tubes fitted with several different DDT enhancing obstacle arrangements demonstrated that for stoichiometric propane-air mixtures, it was not possible to achieve detonations from a weak spark in a practical distance. Furthermore, tests conducted with more sensitive mixtures to allow for early DDT

showed that the presence of obstacles significantly lowers the measured impulse. Higgins et al.[4] showed that even by enriching stoichiometric propane-air mixtures with oxygen and acetylene, the distance over which DDT occurred could not be reduced to less than 1.5 meters. Thus, initiation systems involving DDT alone are unappealing for use in PDEs due to inherent obstacle drag or the long tubes necessary for DDT.

Another technique for initiating detonations in insensitive mixtures involves using a driver or predetonator tube. The driver tube contains a sensitive mixture such as propane-oxygen that transitions to detonation in a very short distance after ignition by a weak spark. The fully developed propane-oxygen detonation wave is then propagated into a test section containing an insensitive mixture such as propane-air. It is possible for the hot products to initiate a detonation in the insensitive mixture given sufficient driver energy. Recently, Schultz and Shepherd[5] explored the critical diffraction limits for detonation transmission from a driver tube into a test section. Two sets of experiments were conducted: one case with the same mixture in both the driver tube and the test section and one case with a sensitized driver gas exhausting into a less sensitive test section. The presence of a sensitive driver was found to improve the transmission of the detonation into the less sensitive test section gas.

Murray et al.[6] were able to dramatically increase the efficiency of the technique by transmitting the detonation from the driver tube into the test section through an annular orifice. All tests were conducted in a uniform mixture. They reasoned that the annular orifice generated an imploding toroidal wave in the test section. The high pressures and temperatures at the focus of the imploding toroid created a hotspot capable of evolving into a self-sustained detonation wave. The addition of the annular orifice allowed successful detonation transmission for tubes 2.2 times smaller in diameter compared to tubes with simple circular orifices.

Research at Caltech verified this concept while using a sensitized driver gas in an effort to increase the transmission efficiency. With this setup, detonations were achieved in test section mixtures of $C_3H_8$-air at room temperature (298 K). However, detonations were not initiated in $C_3H_8$-air or JP10-air at elevated temperatures (373 K). This loss in performance was attributed to the decrease in energy density of the driver and test mixtures due to gas expansion during heating. A method utilizing a more efficient focusing technique, such as shock wave focusing, is necessary to achieve detonations at higher temperatures in the hydrocarbon-air mixtures of interest.

The following describes a program designed to maximize transmission efficiency by generating high energy density regions via an imploding toroidal detonation wave. First, research was conducted on detonation propagation through small tubes. This determined the minimum tube diameter (and thus gas volume) necessary to propagate stable detonation waves. Second, a device capable of generating a planar detonation wave was developed to verify that multiple detonation fronts initiated from a weak spark and propagated through small tubes could be merged to create a detonation wave with a planar front. Finally, a low-drag initiator system capable of producing a repeatable, high-pressure focal region with a minimum amount of driver gas was built using experience gained from small tube and planar initiator data.

## Initiator Development

### Small Tubes

In order to minimize the amount of sensitive driver gas used in detonation initiators, the initiator volume should be as small as possible. However, as the length scale of the initiator approaches the order of the cell size of the mixture, losses due to boundary layer effects can become significant. Such losses can cause the detonation wave to fail or weaken enough to interfere with the operation of the initiator. Thus, knowledge of minimum tube diameters and minimum initial pressures necessary to avoid boundary layer effects is crucial for design of an efficient system.

Researchers such as Manzhalei[7,8] have identified and characterized modes of detonation propagation through small tubes using acetylene-oxygen mixtures. However, limited information is available on the regime of stable propagation of propane-oxygen-nitrogen mixtures. It was necessary to carry out experiments to establish the stable detonation regimes for propagating propane-oxygen detonations in order to optimize our initiator design.

A detonation wave was initiated in a driver tube and propagated into a small tube test section. The small tube test section was equipped with three pressure transducers to allow for velocity and pressure measurements. Test sections of 1.27 mm and 6.35 mm inner diameters were used. Propane-oxygen mixtures were tested, varying the initial pressure and equivalence ratio. Data indicated that significant (>10%) velocity deficits were present when the ratio of induction distance to tube radius was greater than 0.1. This corresponded to a tube diameter of 1.27 mm for stoichiometric propane-oxygen mixtures at 1 bar.

The experiments determined the minimum tube diameter possible to propagate a detonation through a straight uninterrupted tube. The inclusion of corners, bifurcating channels, and other features in an actual initiator necessitates larger tube diameters in order to ensure successful detonation propagation.

### Planar Initiator

A device capable of producing a planar detonation wave was successfully built and tested to demonstrate

the principles of merging a series of wave fronts into a single front. Similar techniques have been used in high explosive research.[9] This device served as a stepping-stone in the development of the toroidal wave generator discussed below. The planar initiator is capable of producing a large aspect ratio, planar detonation from a weak spark.

The planar version, shown in Figure 1, consists of a main channel with secondary channels branching off the main channel. All secondary channels terminate on a line and exhaust into a common test section area. The channel geometry is such that all path lengths from the spark point to the secondary channel termination line are equal. For use with propane-oxygen mixtures, the main channel width was 9.53 mm and 0.431 m. The width of the secondary channels was 5.08 mm and the secondary channel spacing was 2.54 mm. All channels were square in cross-section. The channels exhausted into a test section 0.305 m wide and 0.152 m long. The test section contained a ramp near the secondary channel exhaust that enlarged the channel depth from 5.08 mm to 19.05 mm over a distance of 38.1 mm. The device was filled with premixed propane-oxygen and ethylene-oxygen mixtures. A spark plug and associated discharge system with 30 mJ of stored energy was used to ignite the combustible mixture.

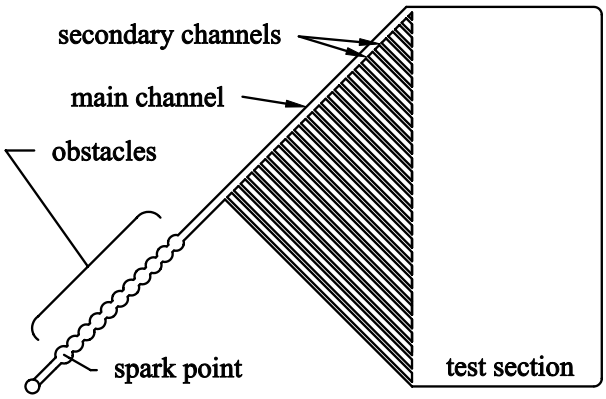


**Fig. 1 Planar initiator schematic.**

The presence of obstacles in the main channel promoted DDT before the reaction front reached the secondary channels, resulting in a detonation that traveled down the main channel with small fronts branching off and traveling down the secondary channels. All detonation fronts exhausted into the test section at the same time and combined to form a planar detonation front. Images and pressure traces show that the device produces planar waves with wave front deviations of less than 1 mm over the width of the test section. The results are extremely repeatable. Chemiluminescence images of the detonation front are shown in Figure 2. These were obtained by using an intensified CCD camera with an exposure time of 100 ns. The detonation luminosity was directly imaged through a clear polycarbonate cover on the planar initiator. The planar initiator was successful in generating planar detonation waves with large aspect ratios.

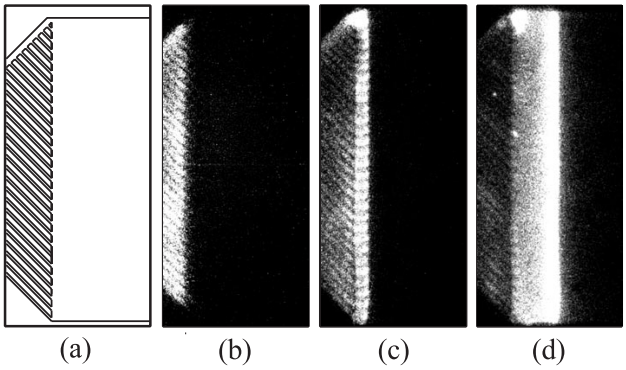


**Fig. 2 Planar initiator results showing: a) schematic of imaging area along with images taken b) 360 $\mu$s, c) 370 $\mu$s, and d) 375 $\mu$s after ignition. Each image was taken during a separate experiment. Test mixture was stoichiometric propane-oxygen at 1 bar.**

**Toroidal Initiator**

To create a toroidal wave, the planar initiator design was modified such that the exit of each channel lies on a circle with the channels exhausting inwards. This involved mapping the planar design onto a cylinder, creating an annular imploding wave as shown in Figure 3. The mapping transforms the metal substrate containing the channels into an inner sleeve while the cover plate becomes the outer sleeve. Creation of a pressure seal between the inner and outer sleeves was accomplished by a shrink fit.[10] All initiator channel dimensions are similar to that of the previously described planar initiator. The small channels exhaust into a test section that is 76.2 mm in diameter. This design allows the initiator to be incorporated into the walls of a PDE. Since no part of the initiator is inside the flow path, drag losses are expected to be minimal in PDE applications.

Testing was performed with stoichiometric propane-oxygen mixtures initially at 1 bar. The device was filled using the method of partial pressures. The mixture was circulated to ensure homogeneity using a bellows pump which limited the initial mixture to pressures of 1 bar or greater. Pressure history was obtained at locations near the focus of the collapsing torus by four pressure transducers, one of which was placed as close to the implosion axis as possible.

The pressure transducers were mounted on a surface that was 19 mm from the center of the exit of the initiator as shown in Figure 3b. The transducers were equally spaced 10.7 mm apart on a radial line with the central transducer located on the central axis of the initiator tube. A typical set of pressure traces is shown in Figure 4.

The outermost three pressure transducers show a

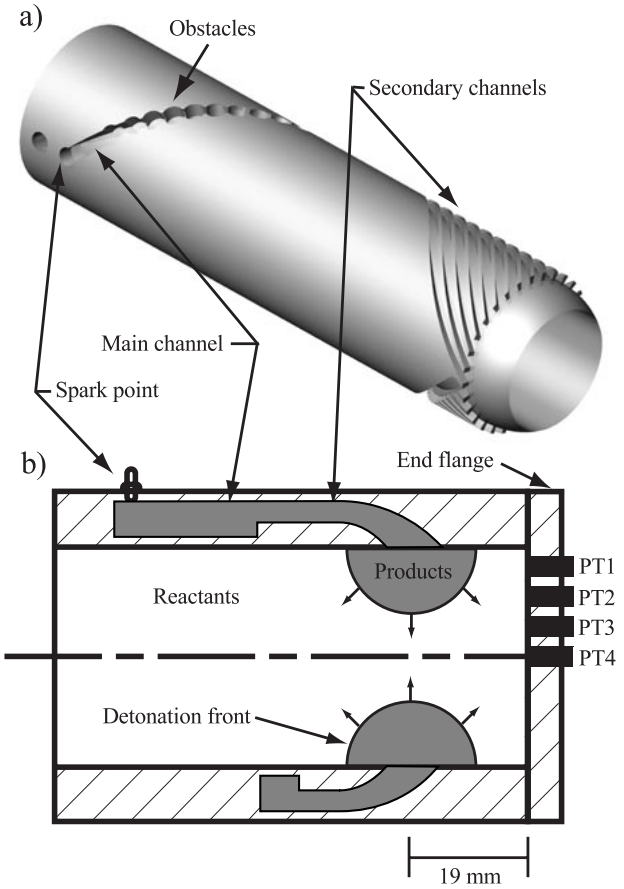


**Fig. 3 Toroidal initiator concept a) rendering and b) accompanying cut-away schematic. In the schematic the grey areas are products, the white section is reactant, and the hatched areas are initiator walls. Pressure transducers are labeled PT1, PT2, PT3, and PT4.**

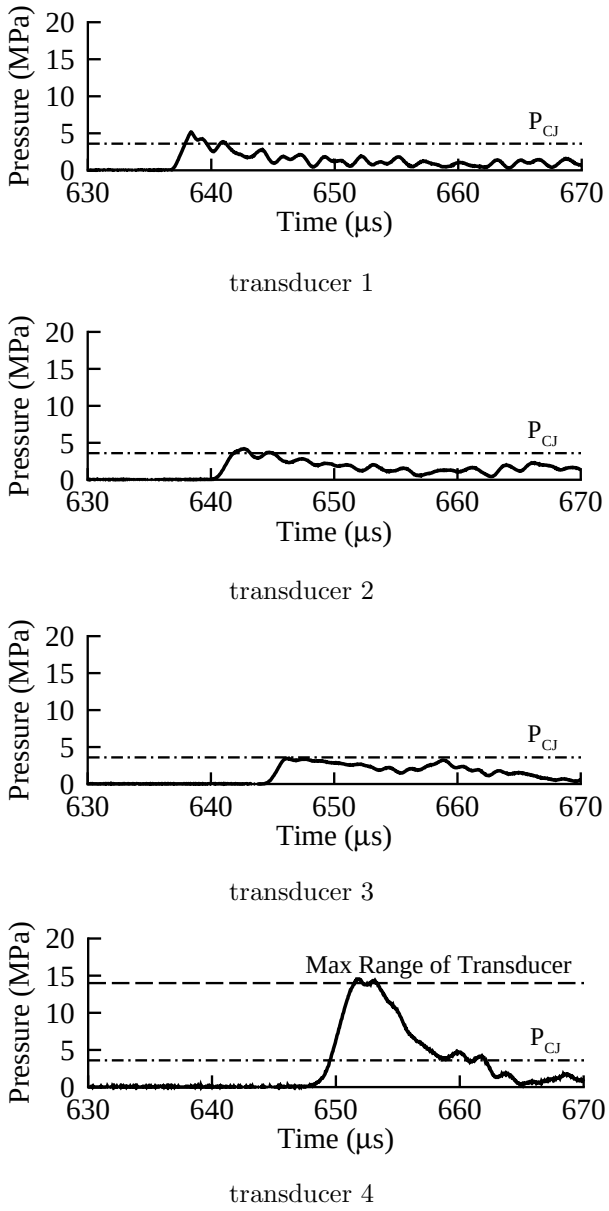


**Fig. 4 Typical pressure traces from a stoichiometric propane-oxygen test. Initial pressure was 1 bar. Location of the pressure transducers is shown in Fig. 3b. The CJ pressure for the mixture is shown as a dashed line. Note that pressure trace 4 exceeds the max reliable range of the transducer.**

gradually decreasing pressure wave amplitude as the radius of the imploding torus, $R_s$ (defined in Figure 6) decreases. However, the pressure apparently rapidly increases between gauges 3 and 4 as the central pressure transducer recorded a value above its maximum reliable operating range. This value was four times larger than the CJ pressure for the mixture. As discussed below, the pressure data differ significantly from theory. The difference is attributed to two effects: shock-wall interactions and diffraction of the toroidal wave.

In order to image the detonation front, the pressure transducer end flange shown in Figure 3 was replaced with a composite window. The inner portion of the window consisted of a thin 3-6 mm sacrificial sheet of glass or optically clear polycarbonate. A 25.4 mm thick optically clear polycarbonate window was clamped against the outside of the sacrificial window. The sacrificial window was used to shield the 25.4 mm thick structural window from the high-temperature combustion products. Glass sacrificial windows failed readily, necessitating replacement every test. Sacrificial polycarbonate windows were rapidly charred by the high-temperature products and were replaced every three to four tests.

An intensified CCD camera was used to take 100 ns exposures of the front. The camera was placed on the centerline of the initiator (the dashed line in Figure 3b) a short distance outside the viewing window. A pressure transducer, mounted at the exhaust of one of the secondary channels, acted as the camera trigger. Images of the detonation front luminosity were also obtained. A series of images of the collapsing detonation wave is shown in Figure 5.

The outermost black portion of each image is the initiator wall, which frames a 76 mm testing area cross-section. In each image, the innermost circle corresponds to the collapsing detonation front. In some images, a curious "flower-shaped" structure behind the collapsing front (between the innermost circle and the initiator wall) is also visible. The structure is not currently understood. It is possible that it is a result of the pressure wave interacting with the polycarbonate window and modifying its optical properties.

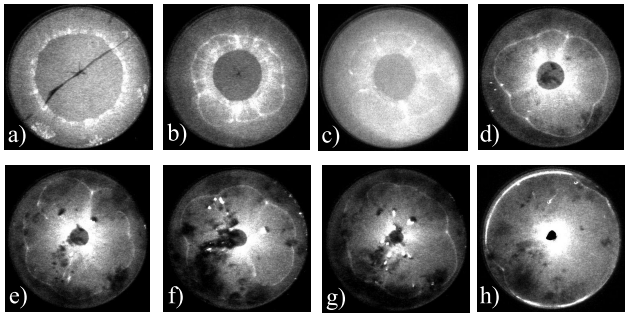


**Fig. 5 Chemiluminescence images of the collapsing toroidal detonation wave. Each image was taken during a separate experiment with a stoichiometric propane-oxygen mixture at 1 bar initial pressure. The period between arrival of the detonation front at the triggering pressure transducer and imaging was a) 29 $\mu$s, b) 34 $\mu$s, c) 35 $\mu$s, d) 37 $\mu$s, e) 38 $\mu$s, f) 38 $\mu$s, g) 39 $\mu$s, h)42 $\mu$s. The dark splotches appearing in images d, e, f, g, and h are due to charring of the polycarbonate window. The black line in image a) is a crack in the glass window.**

## Analysis of the Toroidal Initiator

While scant analysis has been published on imploding toroidal waves,[11] work has been done on cylindrical waves[12–16] due to the simplicity of the geometry. It is possible to imagine approximating the focal region of an imploding toroidal wave as an imploding cylindrical wave. The following analysis assumes first that this approximation is valid, and then compares the result to an approximate solution for an imploding toroidal wave. Experimental results from the toroidal initiator are compared with the approximate cylindrical and toroidal imploding detonation wave solutions. A numerical simulation is then used to help explain the differences between the two cases.

Early research on imploding cylindrical waves focused on shock waves. In 1958, Whitham[17]developed a simple approximate solution to model the shock motion for a cylindrical imploding shock wave. His solution was based on an area-Mach number relationship for a wave and derived by applying the equations of motion along a $C^+$ characteristic to flow behind the wave. The shock motion, pressure, and density can then be obtained using the shock-jump relations. The result shows an inverse relationship between shock speed and shock area. As a shock wave's area decreases, the wave becomes increasingly overdriven, exhibiting elevated post-shock pressures and flow velocities.

Whitham's work was extended by Lee[18] for detonations and used to analyze cylindrically imploding detonation waves, comparing the solution with experiments. Good agreement was found between experiment and theory, demonstrating that a collapsing cylindrical detonation wave is capable of producing pressures about 18 times higher than the normal CJ pressure.

For an imploding cylindrical detonation wave, Lee[18] shows that the Whitham model can be reduced to

$$\frac{1+\gamma\alpha+\gamma\left[(1+\gamma)(1-\alpha)\right]^{\frac{1}{2}}}{(1-\gamma\alpha)(1+\gamma)^2} \cdot\left[1+\gamma\alpha+\left(\frac{1+\gamma\alpha}{1-\alpha}\right)^{\frac{1}{2}}\right]d\alpha+\tfrac{dA}{A}=0\,, \qquad (1)$$

with $\alpha$ in Eq. (1) being used as the variable to describe the normalized wave speed, $\dot{R}_s/D$:

$$\alpha=\left[1-\left(D/\dot{R}_s\right)^2\right]^{\frac{1}{2}}/\gamma\,. \qquad (2)$$

$D$ is the CJ detonation wave velocity,

$$D=\left[2Q\left(\gamma^2-1\right)\right]^{\frac{1}{2}} \qquad (3)$$

in the "strong-shock" limit.

It is necessary to solve Eq. (1) for the wave radius, $R_s$. This can be done by first calculating the inverse ratio of the surface area of a collapsing cylindrical wave, $A$, to its derivative, $dA$, as a function of the normalized shock radius, $R_s/R_i$. $R_i$ is the radius of the detonation wave at CJ conditions

$$dA/A=d(R_s/R_i)\,/\,(R_s/R_i)\,. \qquad (4)$$

Equation (4) is then substituted into the last term of Eq. (1). The result is a differential equation in which the shock radius can be solved as a function of $\alpha$. The boundary condition

$$\frac{R_s}{R_i}=1 \qquad \text{at} \qquad \alpha=0 \qquad (5)$$

can be used assuming that the initial wave is a CJ detonation.

Solving Eq. (1) for $\alpha$ as a function of $R_s/R_i$ allows the density, velocity, and pressure of the collapsing cylindrical detonation wave to be obtained as a function of $R_s/R_i$ from the shock-jump conditions:

$$\frac{\rho}{\rho_i} = \frac{1}{1-\alpha}\,, \qquad (6)$$

$$\frac{u}{u_i} = \frac{1+\gamma\alpha}{(1-\gamma^2\alpha^2)^{\frac{1}{2}}}\,, \qquad (7)$$

$$\frac{p}{p_i} = \frac{1}{1-\gamma\alpha}\,. \qquad (8)$$

It is also possible to approximate the motion of an imploding toroidal detonation wave using this method. Equations (1)-(3) and (6)-(8) remain valid as they are geometry independent. However, Eq. (4) needs to be adapted to the toroidal geometry.

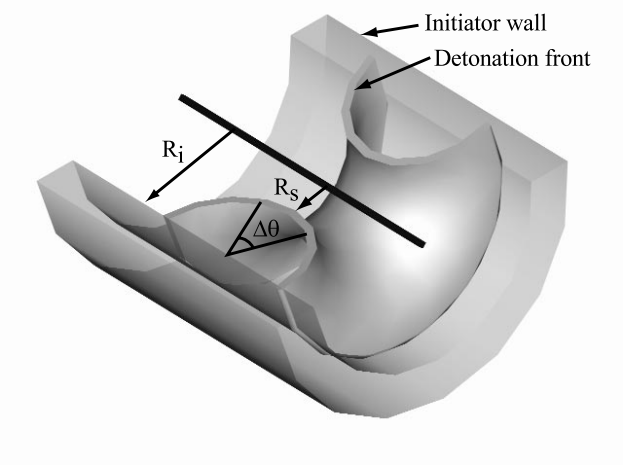


**Fig. 6 The geometry of the toroidal detonation front.**

For the geometry of Figure 6, the differential area of a central element of the imploding toroidal detonation wave front initiated at a circle of radius, $R_i$, can be represented as

$$\Delta A = 2\pi R_s \cdot \Delta\theta \left(R_i - R_s\right) . \tag{9}$$

This is the equation for a parabola. Thus, as the $R_s$ decreases (corresponding to an increase of the radius of the torus), the differential surface area of a central element of the front first increases to a maximum at $R_s = R_i/2$ then decreases. With $A$ represented as a function of $R_s$, $dA/A$ can be represented in terms of $R_s/R_i$. However, directly solving for the flow as was done in the cylindrical case is not possible without an additional assumption that the detonation wave remains at CJ conditions throughout that region of increasing area ($R_s/R_i = 0 \rightarrow 0.5$). This is necessary since there are no solutions to the Whitham model (Eq. 1) when $\dot{R}_s < D$.

Experimentally, a CJ wave emerging from the annulus at $R_i$ could fail, becoming a non-reactive shock as its area increases. While it is possible that the resulting decoupled shock and reaction zone could reinitiate a detonation following the region of area increase, such analysis is beyond the scope of this paper. Instead, it is assumed that the detonation is ideal and remains at the CJ condition throughout the area expansion process. Whitham's method is applied only to the wave from $R_s/R_i = 0.5 \rightarrow 1$. In this regime, area is decreasing, resulting in an overdriven ($\dot{R}_s > D$) detonation wave.

In practice, the likelihood of failure depends on the speed of the emerging detonation and the thickness of the detonation reaction zone as compared to the annular opening. While no results are available in the literature for diffraction of waves through an annulus in the side wall of a tube, Murray et al.'s[6] results for an annular opening at the end of a tube should be a useful guide. If the detonation is propagating close to the CJ velocity, it will be transmitted as a detonation if the reaction zone length is sufficiently small compared to the width of the annular opening. If the reaction zone is too thick in comparision to the annular opening, failure of the detonation diffraction is anticipated. In the present case, the annular opening is about 12.7 mm, which is 423 times larger than the estimated reaction zone length[19] of 30 $\mu$m for a stoichiometric propane-oxygen mixture at an initial pressure of 1 atm. Based on previous diffraction experiments with slots,[20] this should be adequate to get successful detonation. In terms of the more conventional approach using detonation cell width to characterize the opening, the cell width is about 0.9 mm and the opening is therefore about 14 cell widths, greater than the six to ten cell widths previously observed[20] to be needed for successful diffraction from planar slots.

Experimental pressure data for the toroidal wave are plotted against previously discussed cylindrical and toroidal theories and shown in Figure 7. As exhibited in the pressure history data in Figure 4, the pressure of the toroidal detonation wave initially decays before increasing to more than four times $P_{CJ}$ during the final stages of focusing. As expected, neither the cylindrical theory nor the toroidal theory exhibits any pressure decay at any point during the focusing process.

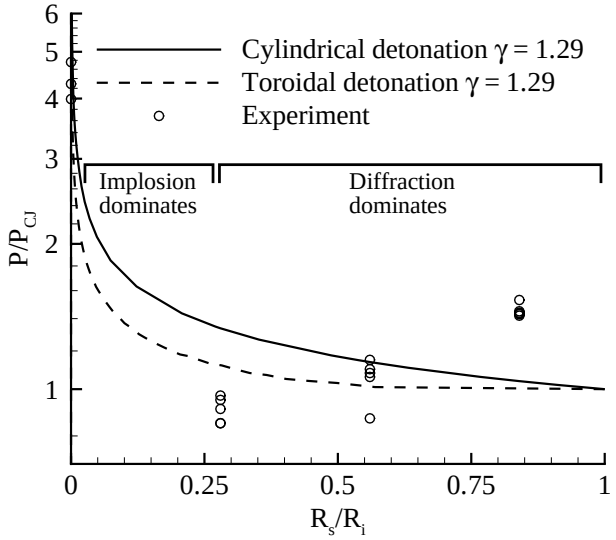


**Fig. 7 Comparison of imploding cylindrical detonation theory, imploding toroidal detonation theory, and experimental data.**

It is important to note that, as shown in Figure 3, pressure was not actually measured along the central axis of the toroidal implosion, where the theoreti-

cal cylindrical and toroidal pressures were calculated. Thus, the measured pressures do not directly compare to the idealized calculations. Instead, they show effects of off-axis diffraction and shock interaction with the pressure measurement wall. The peak pressures measured by the transducers on the end flange of the initiator are significantly influenced by the angle the detonation wave makes with respect to the surface. Only when the detonation front is normal to the wall can pressure be considered representative of the actual pressure in the undisturbed waves. The geometric considerations and the wave front shapes computed in the shock simulation of Figure 8 discussed below indicate that a range of obliquities occurs. At the outer edge of the flange, the wave front is almost parallel to the end flange. As the wave proceeds inward, the front will rotate away from the wall. Previous work[16,21,22] has shown that the reflection type will change from regular reflection to Mach reflection at the point where the included angle between the wave front and the wall is about 55°. For included angles between 0° and 55°, the peak pressure will be approximately 2.5 $P_{CJ}$. Between 55° and 90°, the pressure decreases monotonically to $P_{CJ}$. This variation of pressure with wave angle is responsible for the peak pressure values greater than CJ which are observed on the outer two transducers.

A computer simulation of the experiment was used to help clarify the pressure wave interactions and focusing phenomenon. Hornung[23] computationally[24] simulated a strong shock propagating through the geometry of the toroidal initiator. Although the simulation is for unreacting flow, it demonstrates how shock interaction with the pressure-sensing wall can result in the observed pressures. A series of images of the simulated shock geometry and pressure profile along the right wall is shown in Figure 8. The simulation assumes an ideal gas in two-dimensional, axisymmetric flow; the lower edge of each image is the axis of symmetry.

The simulation captures the experimental trend with initial pressure decay and the following large increase in pressure towards the end of the focusing process. Figure 9 is a composite of several images showing the leading shock at four different times along with the locations of the pressure transducers in the experiment. Also shown are portions of the pressure wave for each shock front shown. A line indicating the leading shock pressure as a function of location is also present. Note the interaction of the shock with the wall at each location.

Initially, near transducer P1, the shock wave exhibits almost complete normal reflection from the wall. Correspondingly, the measured pressure at location P1 is higher than the initial shock pressure. As the wave progresses, the reflection develops into a small Mach stem at location P2, which results in a lower measured

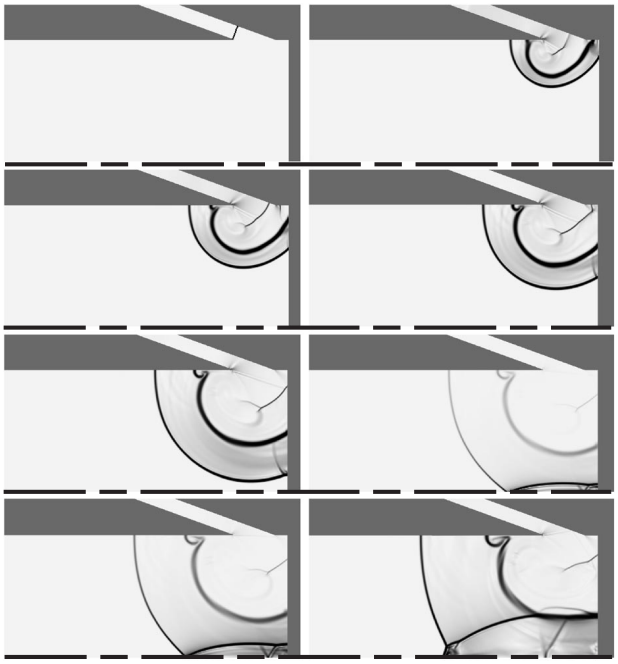

**Fig. 8 A series of images from numerical computations showing an imploding toroidal shock wave. The images are pseudo-schlieren visualizations showing density gradients in the flow. The initial conditions were a shock wave with $P_2/P_1 = 15$ and $T_2/T_1 = 10$. Computations by Hornung[23] using Amrita.[24]**

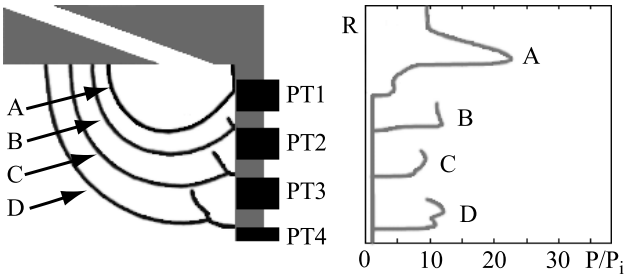


**Fig. 9 This composite image shows the shock front at four different times. The corresponding special pressure profiles are also plotted.**

pressure than was recorded at P1. As the Mach stem increases in size, the measured pressure at the wall decreases. Between locations P3 and P4, the focusing processes, initially weak, begin to dominate the system, and the pressure rises dramatically.

The measured pressure evolution can be thought of as a combination of three processes: detonation-wall interaction, focusing effects, and diffraction losses. Initially, the detonation is not overdriven and focusing effects are weak. Detonation-wall interactions dominate the measured pressure, leading to the apparent pressure decay. Later on in the process after Mach stem has developed, focusing processes significantly overdrive the wave, dramatically increasing the pressure. It is important to note that the apparent pressure decay due to the wall reflection is not actually present

along the focal axis of the device, whereas the pressure increase due to focusing is present. However, since the toroidal wave is diffracting, some pressure decay is expected at any location off the implosion axis. Neither the diffraction losses nor the apparent wall reflection losses are present in the theoretical cylindrical wave solution as the wave is always perpendicular to the pressure wall.

## Summary and Conclusion

Devices capable of producing imploding toroidal waves and planar detonation waves from single weak sparks have been constructed. The toroidal wave initiator should be appealing to designers of PDEs due to the low-drag design, low energy requirements, and optimized use of sensitized driver gas. The planar initiator should be useful in laboratory experiments to produce a planar detonation front in channels with large aspect ratios.

Analysis of experimental data and comparison with theory and simulations confirmed that the toroidal initiator is capable of producing a high-pressure focal region. Future work will focus on pulsed operation of the toroidal and planar initiators.

## Acknowledgment

The authors are extremely grateful to H. Hornung for his numerical modeling of the toroidal initiator. They would also like to thank M. Grunthaner for his assistance with the design of the toroidal initiator, J. Haggerty and B. St. John for their expertise and patience during initiator construction, and F. Pintgen for his assistance in carrying out some of the experiments.

This work was supported by the Office of Naval Research Multidisciplinary University Research Initiative *Multidisciplinary Study of Pulse Detonation Engine* (grant 00014-99-1-0744, sub-contract 1686-ONR-0744), and General Electric contract GE-PO A02 81655 under DABT-63-0-0001.

## References

[1]Brophy, C. M. and Netzer, D. W., "Effects of Ignition Characteristics and Geometry on the Performance of a JP-10/$O_2$ Fueled Pulse Detonation Engine," 35th AIAA/ASME/SAE/ASEE Joint Propulsion Conference and Exhibit, June 20–24, 1999, Los Angeles, CA, AIAA 99-2635.

[2]Brophy, C., Sinibaldi, J., and Damphousse, P., "Initiator Performance for Liquid–Fueled Pulse Detonation Engines," 40th AIAA Aerospace Sciences Meeting and Exhibit, January 14–17, 2002, Reno, NV, AIAA 02-0472.

[3]Cooper, M., Jackson, S., Austin, J., Wintenberger, E., and Shepherd, J. E., "Direct Experimental Impulse Measurements for Deflagrations and Detonations," 37th AIAA/ASME/SAE/ASEE Joint Propulsion Conference, July 8–11, 2001, Salt Lake City, UT, AIAA 2001-3812.

[4]Higgins, A., Yoshinaka, P., and Lee, J., "Sensitization of Fuel-Air Mixtures for Deflagration to Detonation Transition," *Proceedings of the International Colloquium on Control of Detonation Processes*, Moscow, Russia, July 4-7, 2000.

[5]Schultz, E. and Shepherd, J., "Detonation Diffraction through a Mixture Gradient," GALCIT Technical Report FM00-1, Graduate Aeronautical Laboratories, California Institute of Technology, Pasadena, CA 91125, 2000.

[6]Murray, S., Thibault, P., Zhang, F., Bjerketvedt, D., Sulmistras, A., Thomas, G., Jenssen, A., and Moen, I., "The Role of Energy Distribution on the Transmission of Detonation," *Proceedings of the International Colloquium on Control of Detonation Processes*, Moscow, Russia, July 4-7, 2000.

[7]Manzhalei, V., "Detonation Regimes of Gases in Capillaries," *Fizika Goreniya i Vzryva*, Vol. 28, No. 3, 1992, pp. 93–99.

[8]Manzhalei, V., "Low-Velocity Detonation Limits of Gaseous Mixtures," *Combustion, Explosion, and Shock Waves*, Vol. 35, 1999, pp. 296–302.

[9]Hill, L., private communication, 2000.

[10]Grunthaner, M., Jackson, S., and Shepherd, J., "Design and Construction of an Annular Detonation Initiator," GALCIT Technical Report 2001.005, Graduate Aeronautical Laboratories, California Institute of Technology, Pasadena, CA 91125, 2001.

[11]Jiang, Z. and Takayama, K., "Reflection and focusing of toroidal shock waves from coaxial annular shock tubes," *Computers and Fluids*, Vol. 27, No. 5-6, 1998, pp. 553–562.

[12]Takayama, K., Kleine, H., and Gronig, H., "An Experimental Investigation of the Stability of Converging Cylindrical Shock Waves in Air," *Experiments in Fluids*, Vol. 5, No. 5, 1987, pp. 315–322.

[13]Devore, C. and Oran, E., "The Stability of Imploding Detonations in the Geometrical Shock Dynamics (CCW) Model," *Physics of Fluids*, Vol. A4, No. 4, 1992, pp. 835–844.

[14]Oran, E. and Devore, C., "The Stability of Imploding Detonations - Results of Numerical Simulations," *Physics of Fluids*, Vol. 6, No. 1, 1994, pp. 369–380.

[15]Terao, K., Akaba, H., and Shiraishi, H., "Spherically imploding detonation waves initiated by 2-step divergent detonation," *Shock Waves*, Vol. 4, No. 4, 1995, pp. 187–193.

[16]Akbar, R., *Mach Reflection of Gaseous Detonations*, Ph.D. thesis, Rensselaer Polytechnic Institute, Troy, New York, 1997.

[17]Whitham, G., "On the propagation of shock waves through regions of non-uniform area or flow," *Journal of Fluid Mechanics*, Vol. 4, 1958, pp. 337–360.

[18]Lee, J. and Lee, B., "Cylindrical Imploding Shock Waves," *The Physics of Fluids*, Vol. 8, No. 12, 1965, pp. 2148–2152.

[19]Schultz, E. and Shepherd, J., "Validation of detailed reaction mechanisms for detonation simulation," GALCIT Technical Report FM99-5, Graduate Aeronautical Laboratories, California Institute of Technology, Pasadena, CA 91125, 2000.

[20]Benedick, W., Knystautas, R., and Lee, J., "Large scale experiments on the transmission of fuel-air detonations from two-dimensional channels," *Dynamics of Detonations and Explosions*, Vol. 94 of *Prog. Astro. Aero.*, AIAA, New York, 1984, pp. 546–555.

[21]Nettleton, M. A., *Gaseous Detonations*, Chapman and Hall, 1987.

[22]Meltzer, J., Shepherd, J. E., Akbar, R., and Sabet, A., "Mach Reflection of Detonation Waves," *Dynamics of Detonations and Explosions*, Vol. 153 of *Prog. Astro. Aero.*, AIAA, New York, 1993, pp. 78–94.

[23]Hornung, H., private communication, 2002.

[24]Quirk, J., "AMRITA - A Computational Facility (for CFD Modelling)," VKI 29th CFD Lecture Series, ISSN 0377-8312, 1998.